Available online at www.sciencedirect.com
SCIENCE DIRECT®
International Journal of Mass Spectrometry 228 (2003) 1083–1093
International Journal of Mass Spectrometry
www.elsevier.com/locate/ijms

Fragmentations of some dinitrile anions

Gustav Bojesen[a,1], Einar Uggerud[b,*]

[a] *Department of Chemistry, University of Copenhagen, DK-2100 Copenhagen, Denmark*
[b] *Department of Chemistry, University of Oslo, P.O. Box 1033, Blindern, N-0315 Oslo, Norway*

Received 13 December 2002; accepted 1 May 2003

Dedicated to Prof. Dr. Helmut Schwarz on the occasion of his 60th birthday.

Abstract

The anions formed by deprotonation of heptane-, octane- and nonanedinitriles have been investigated using mass analyzed ion kinetic energy (MIKE) spectrometry with and without collisional activation. In addition, high level quantum chemical calculations have been used to model relevant parts of the potential energy surfaces. These models are in good agreement with the experimental findings. The lowest energy fragmentations are due to bond scissions initiated by intramolecular hydrogen rearrangements. The calculations show that formation of the enamine anion which is an intermediate in the Thorpe–Ziegler reaction occurs via a high barrier.

Keywords: Metastable ions; MIKE-spectrometry; Quantum chemistry; Chemical ionization; Fast atom bombardement; Reaction mechanisms

1. Introduction

Most unfunctionalized alkyl anions in the gas phase are unstable towards electron loss, and stable alkyl anions are generally stabilized by α-substitution with an electron-withdrawing group. However, the cyano group can stabilize a negative charge in the β-position [1] as well as in the α-position [2–4]. The present work describes the results from computational and experimental investigations of the fragmentation of anions from medium-chained dinitriles. In fast atom bombardment (FAB) ionization such compounds are suitable solvents for strongly oxidizing samples [5].

In solution, base-catalyzed self-condensation of nitriles, also known as the Thorpe reaction, leads to cyano imines which tautomerizes to enamines [6]. The refined intramolecular version of this reaction is known as the Ziegler method and is especially used in the synthesis of cyclic ketones [7]. The initial step in the reaction is similar to the Dieckmann condensation in that a stabilized carbanion attacks an electrophilic multiply bonded carbon. When this is an ester functionality, substitution can follow—a possibility lacking in the case of a nitrile. The Dieckmann condensation is well known to take place in the gas phase [8,9].

2. Experimental methods

The measurements were done on a JEOL (Tokyo, Japan) JMS-HX110/HX110A which is a four-sector

* Corresponding author. Tel.: +47-22-85-55-37; fax: +47-22-85-54-41.
E-mail addresses: bojesen@kiku.dk (G. Bojesen), einar.uggerud@kjemi.uio.no (E. Uggerud).
[1] Co-corresponding author.

1387-3806/$ – see front matter © 2003 Elsevier Science B.V. All rights reserved.
doi:10.1016/S1387-3806(03)00268-9

tandem mass spectrometer with $E_1B_1E_2B_2$ geometry. The anions were generated by FAB or chemical ionization (CI) from the pure dinitriles. The dinitriles were supplied by Aldrich and used as delivered. FAB was done with Xe at 3 kV, and CI with a mixture of CH_4 and N_2O at a ratio of approximately 2:1. With CI, heptane- and octanedinitrile can be introduced directly or via a heated reservoir whereas nonanedinitrile also can be introduced directly. The resolving power of the mass spectrometer was set to 1000 and the accelerating potential at 10 kV. The potential on the post acceleration detector was 20 kV. The dissociation products of the anions were detected by mass analyzed ion kinetic energy (MIKE) spectrometry in which the parent anion was selected by MS1 (E_1B_1). Fragments formed in the 3rd field-free region were registered by an off-axis detector, placed after E_2, by varying the potential of E_2. Data were collected over a period of 10–30 min. In the MIKE experiments the peak-width at half height was measured and corrected for the width of the main beam [10]. The translational energy release ($T_{0.5}$) was determined as described by Cooks et al. [11].

Collisional activation (CA) spectra were obtained by admitting air into a grounded collision cell in the 3rd field-free region. The pressure was adjusted to give 80% transmission of the main beam.

3. Theoretical methods

The program suite GAUSSIAN 98 [12] was employed for all quantum chemical calculations. The hybrid density functional theory method B3LYP according to Becke [13] incorporating the 6-31G(d) basis set [14] was used. All stationary points were subject to complete geometry optimization with B3LYP/6-31G(d). The optimized structures were checked for the correct number of negative eigenvalues of the Hessian (the second derivative matrix). Analytical force constants were computed at this stage and the vibrational frequencies were obtained together with the rotational constants. These molecular parameters were used within the framework of the rigid-rotor/harmonic-oscillator approximation without any empirical correction to calculate the absolute zero point vibrational energies and thermochemical quantities. For selected geometries quadratic configuration interaction calculations were performed, taking single and double excitations explicitly into account for all valence electrons [15]. These QCISD-FC/6-311++G(d,p)//B3LYP/6-31G(d) results represent our best estimates to relative energies of the species involved.

The reliability of methods based on density functional theory has been examined before [1]. For present work the well-known acidities of hydrogen cyanide and acetonitrile may serve as guides to the accuracy of the calculation scheme. By using the absolute enthalpies calculated for CH_3CN, CH_2CN^-, HCN and CN^-, and the absolute enthalpy for H^+ ($5/2 \times RT$), we find the $\Delta_r H^\circ$ for hydrogen cyanide and acetonitrile to be 1464 and 1586 kJ mol^{-1}, respectively. These numbers should be compared with the corresponding experimental figures of 1463±13 and 1560±20 kJ mol^{-1} [16]. On this basis we may assume that relative energies are reproduced quite accurately, probably within 20–30 kJ mol^{-1}.

4. Results and discussion

4.1. MIKE and CA spectra

In Fig. 1a a MIKE-spectrum of octanedinitrile anion obtained using FAB ionization is shown. Comparison with the MIKE-spectra obtained from the analogous heptane- and nonanedinitrile anions shows that the fragmentation strongly depends on the chain-length (Table 1). The peaks shown in Fig. 1a–c are partial MIKE-spectra of octane- and nonanedinitrile anion produced by CI. In the spectrum of heptanedinitrile anion the only fragment is at *m*/*z* 26, and can be assigned to CN^-. In the spectra of octane- and nonanedinitrile the most significant additional peaks are observed at *m*/*z* 40, 52, 94 (octanedinitrile anion) and *m*/*z* 108 (nonanedinitrile anion). For the smallest ions the natural assignments leaves little doubt. Thus *m*/*z* 40 is deprotonated acetonitrile, and *m*/*z* 52 is deprotonated acrylonitrile. Both the peaks at *m*/*z* 94 and

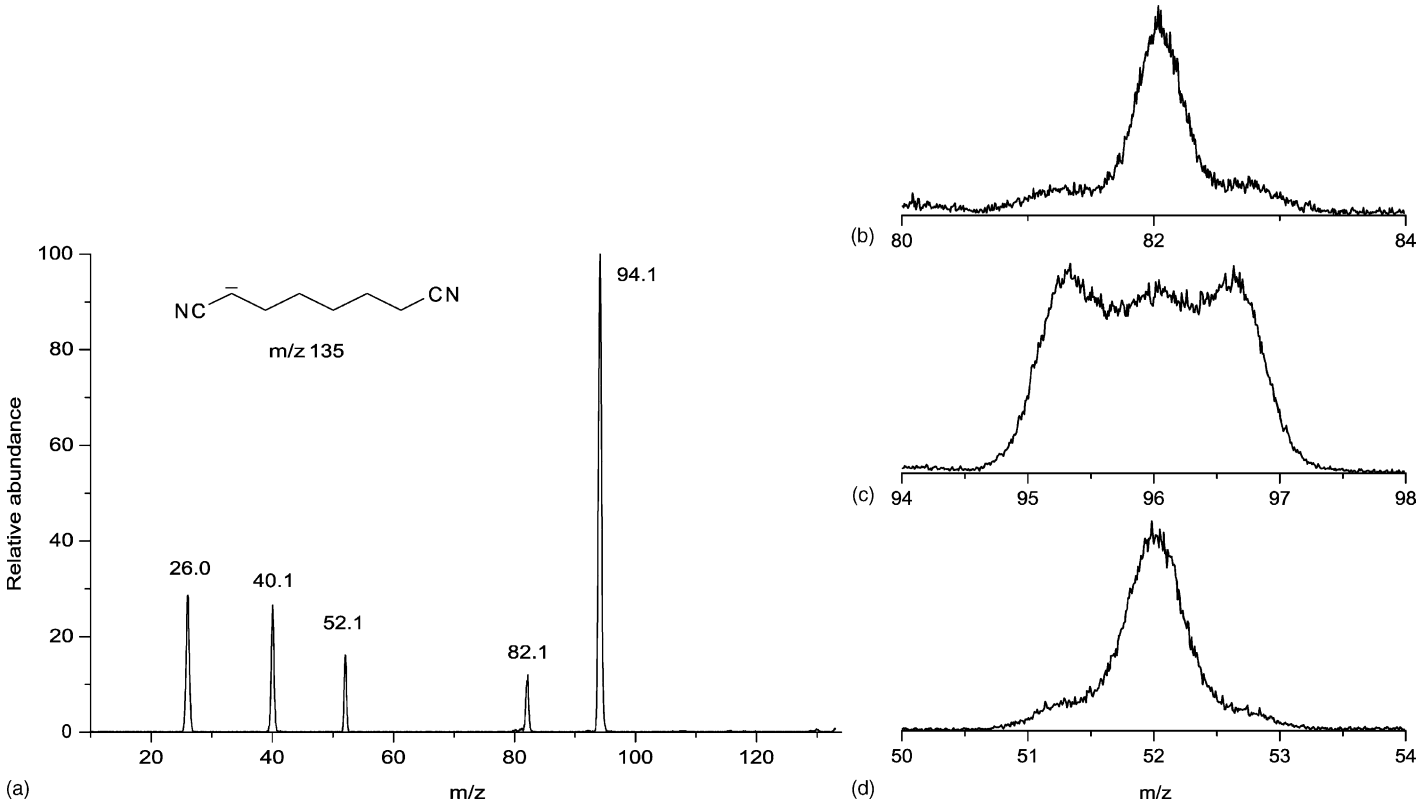

Fig. 1. (a) MIKE-spectrum of octanedinitrile anion formed by FAB. (b) Partial MIKE-spectrum of octanedinitrile anion formed by CI. (c, d) Partial MIKE-spectra of nonanedinitrile anion formed by CI.

Table 1
Summaries of the MIKE-spectra of anions formed by FAB or CI

	Heptanedinitril (*m/z* 121)		Octanedinitrile (*m/z* 135)		Nonanedinitrile (*m/z* 149)	
	FAB	CI	FAB	CI	FAB	CI
m/z 26	100 (59)	100 (86)	29 (60)	74 (87)	37 (74)	60 (87)
m/z 40	Trace	5	27 (24)	85 (91)	36 (31)	78 (92)
m/z 52		Trace	16 (14)	24 (17)	5 (18)	9 (25)
m/z 82			12 (12)	25[a]		
m/z 94			100 (17)	100 (19)		
m/z 96					Trace	36 (212)[b]
m/z 108					100 (20)	100 (31)

The relative abundance of the peaks is given relatively to the most intense peak in the MIKE-spectrum. The translational energy release $T_{0.5}$ (in meV) is given in parentheses. The T value is calculated from the broad component.
[a] Composite peak.
[b] Flat-topped peak.

108 can be assigned to loss of acetonitrile from the parent ions at *m/z* 135 and 149, respectively.

Comparison of the MIKE-spectra of the anion made by FAB and CI shows considerable differences both in the relative intensity of the peaks and in their shapes. For octane- and nonanedinitrile the main differences are the higher abundance of the ion with *m/z* 40 compared to the ions with *m/z* 16 and 52, and higher abundance of the ions with *m/z* 82 (from octanedinitrile anion) and *m/z* 96 (from nonanedinitrile anion).

Most of the peaks-shapes are Gaussian and the peak-widths obtained with both ionization methods were used to obtain the translational energy releases ($T_{0.5}$) as summarized in Table 1. The relative magnitude of the measured translational energy release appears generally to be higher in the spectra obtained with CI than with FAB. When the anions are formed by FAB, the peaks in the MIKE-spectra are Gaussian whereas some of the peaks-shapes are observed to be composite when CI is used. The composite peaks are shown in Fig. 1b–d.

The difference in the MIKE-spectra of the anions formed by CI and FAB may either arise from isomerizations of the anions prior to their decomposition, or from differences in the internal energy of the reacting metastable ions. Support for the latter possibility is provided by the changes observed in the spectra when the anions formed by FAB are collisionally activated.(Table 2) As in the CI MIKE-spectra of both octane- and nonanedinitrile anions, the relative abundance of *m/z* 40 increases compared to those of *m/z* 26 and 52, and the ions with *m/z* 82 (octanedinitrile anion) and *m/z* 96 (nonanedinitrile anion) increase in relative abundance. Significant additional peaks are observed at *m/z* 80 (octanedinitrile anion) and *m/z* 94 (nonanedinitrile anion). At higher collision gas pressures these peaks increase further in intensity.

4.2. Theoretical model

The computational investigation has been concentrated on octanedinitrile anion and the results are summarized in Table 3, Figs. 2 and 3. Due to the

Table 2
Summaries of CA-spectra of dinitrile anions obtained with 80% transmission

	Octanedinitrile anion (*m/z* 135)[a]	Nonanedinitrile anion[b] (*m/z* 149)
m/z 26	35	20
m/z 40	42	45
m/z 52	21	10
m/z 82	18	9
m/z 94	100	
m/z 96		9
m/z 108		100

Intensities are given as percentages of the most intense peak in the spectrum.
[a] A small peak was observed at *m/z* 80.
[b] Small peaks were observed at *m/z* 66, 94 and 132.

Table 3
Energies (in Hartrees) from the quantum chemical calculations

Structure	B3LYP/6-31G(d)	QCISD-FC/6-311++G(d,p)//B3LYP/6-31G(d)	ZPVE	ν(R–C) (**i** cm^{-1})
1	−420.94815	−419.89121	0.17358	–
2	−420.97965	–	0.17587	–
3	−328.12061	–	0.16989	–
4	−92.82453	−92.63856	0.00487	–
5	−420.95330	–	0.17211	–
6	−420.95141	–	0.17170	–
7	−288.17336	–	0.12456	–
8	−132.75493	−132.43007	0.04564	–
9	−288.79791	–	0.14032	–
10	−132.12245	−131.81173	0.03077	–
11	−420.91441	–	0.17041	–
12	−420.94352	–	0.17193	–
13	−328.08705	−327.24055	0.16548	–
14	−420.91131	–	0.17084	–
15	−420.92792	–	0.16876	–
16	−420.93002	–	0.16881	–
17	−288.77175	−288.03153	0.13711	–
18	−288.15115	−287.41692	0.12133	–
19	−420.93015	–	0.16920	–
20	−420.93135	−419.86823	0.16978	–
21	−250.07002	−249.43405	0.11663	–
22	−170.83155	−170.40632	0.05098	–
23	−250.69672	−250.05353	0.13218	–
24	−170.20546	−169.79210	0.03678	–
25	−381.63205	–	0.14452	–
26	−248.83589	–	0.09284	–
27	−249.45899	–	0.10828	–
28	−420.92378	–	0.17536	–
29	−420.98139	−419.92150	0.17813	–
30[a]	−93.42262	−93.21003	0.01646	–
TSA	−420.89556	−419.83511	0.17300	557
TSB	−420.89519	−419.82264	0.17076	511
TSC	−420.94320	–	0.16760	1102
TSD	−420.91385	–	0.16798	450
TSE	−420.89674	−419.84278	0.16914	246
TSF	−420.90872	−419.84754	0.16785	776
TSG	−420.90133	−419.84751	0.16993	72
TSH	−420.91980	–	0.16469	1096
TSI	−420.87230	−419.81064	0.16598	260
TSJ	−420.92123	–	0.16490	1121
TSK	−381.59510	–	0.13926	750
TSL	−381.56515	–	0.13849	1502
TSM	−420.88387	−419.82626	0.17169	1747

[a] HCN.

advantageous interaction with the neighboring partially positive cyano carbon [4], deprotonation of the α-carbon is by far the most favorable in terms of potential energy, and consequently **1** is the energy minimum. The conformation of lowest energy has an intramolecular hydrogen bond. This interaction lowers the potential energy by an extra 15 kJ mol^{-1}, compared to the open chain form. Intramolecular H-bonds are also found in the anions formed by deprotonation of the β- and γ-positions. The corresponding anions

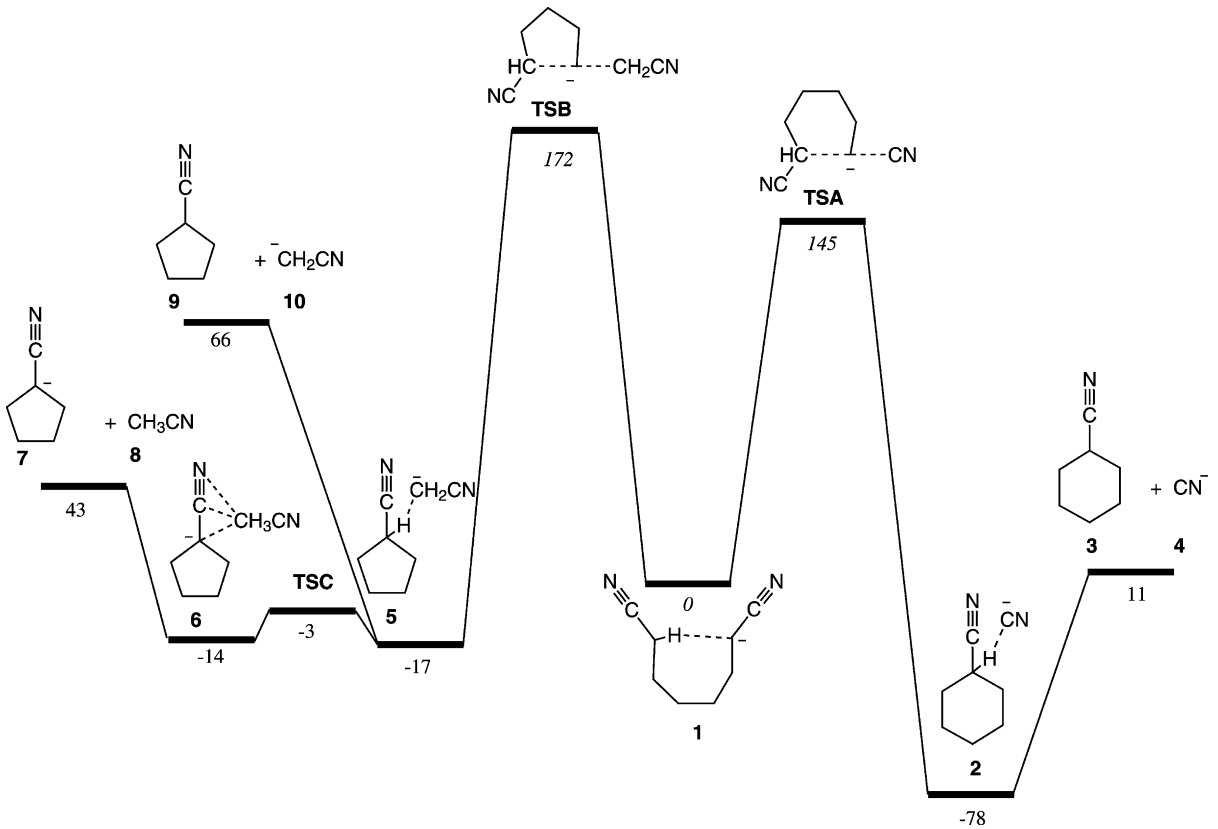

Fig. 2. Unimolecular reactions of octanedinitrile anion (ions with *m*/*z* 26, 40 and 94). Potential energy diagram of the intramolecular S_N2 type reactions (via **TSA** and **TSB**, respectively) giving rise to cyclic products. Numbers in italics correspond to QCISD-FC/6-311++ G(d,p)//B3LYP/6-31G(d), while the numbers in regular font correspond to B3LYP/6-31G(d). Relative energies are given in kJ mol^{-1}.

11 and **14** are 75 and 84 kJ mol^{-1} higher in energy than **1**, respectively. Even without hydrogen-bonding the β-anion is stable towards electron loss [1] and the present results indicate that also a weakly hydrogen-bonded γ-anion is stable in this respect. This intramolecular stabilization could be regarded as an example of remote functionilzation [17]. This idea is not as remote as the critical reader might think, since it is a matter of fact that remote functionalization was introduced for C–H bond activation in nitriles.

Furthermore, the ease of hydrogen rearrangement clearly demonstrates that any attempt of deuterium labeling for the purpose of elucidating the detailed reaction mechanism would be in vain for these molecules.

Observation of ions with *m*/*z* 26 and 40 are assigned to CN^- and CH_2CN^-, indicating fragmentation at the molecular termini. These fragments may be formed by intramolecular S_N2 from the α-anion **1** or by direct fragmentation of the β- and γ-anions **11** and **14**. S_N2 type of mechanisms are well known to play an important role in ion–molecule reactions in the gas phase [18–21].

Fig. 2 shows the calculated potential energy profile for the S_N2 scenario. It is evident that both the anticipated five-membered (**TSA**) and six-membered (**TSB**) transition structures are accessible from **1**. Of these two, **TSA** is lowest in potential energy. Upon formation of CN^- (**4**, *m*/*z* 26) the accompanying neutral fragment is cyclohexyl nitrile (**3**). Due to the high

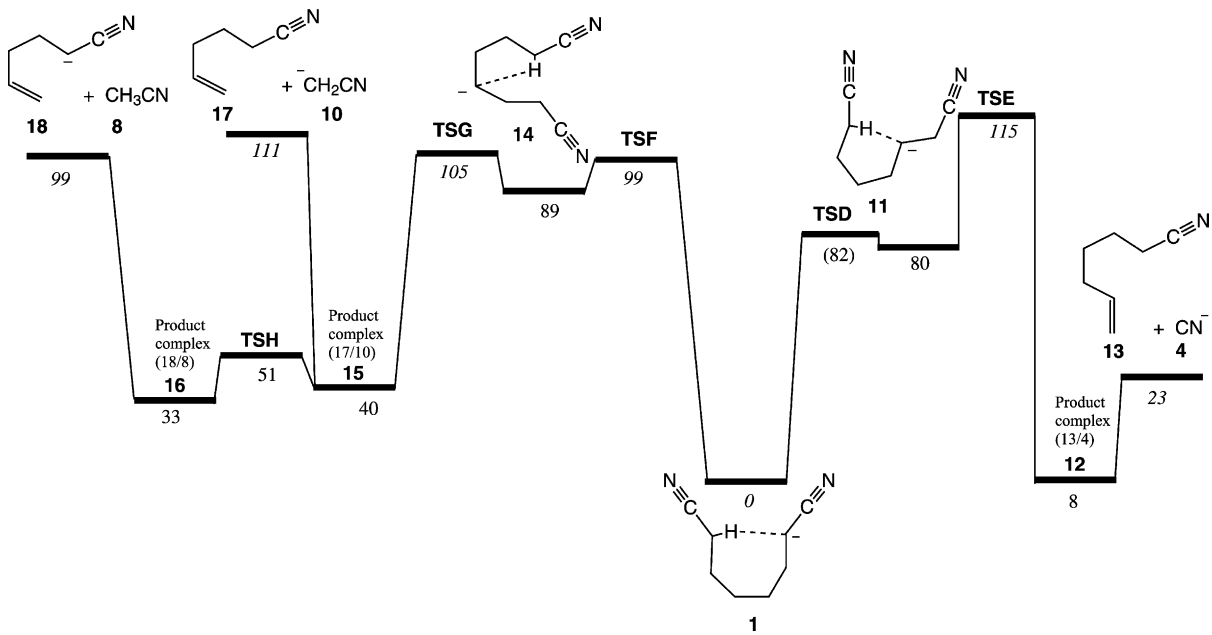

Fig. 3. Unimolecular reactions of octanedinitrile anion (ions with *m*/*z* 26, 40 and 94). Potential energy diagram of the reactions resulting from intramolecular proton transfer, ultimately giving rise to open chained products. Numbers in italics correspond to QCISD-FC/6-311++G(d,p)//B3LYP/6-31G(d), while the numbers in regular font correspond to B3LYP/6-31G(d). Relative energies are given in $kJ\,mol^{-1}$.

acidity of HCN (low $\Delta_r H^\circ$ value), no proton transfer from cyclohexyl nitrile to CN^- is possible, and the anion of the cyclohexyl nitrile is not observed in the experiment. The alternative route via **TSB** ends up with formation of cyclopentyl nitrile (**9**) and CH_2CN^- (**10**, *m*/*z* 40) in one channel, and with the complementary products **7** and **8** (*m*/*z* 94) in the other. Cyclopentyl nitrile is a stronger acid than acetonitrile ($\Delta_r H^\circ = 1560\,kJ\,mol^{-1}$), so the latter pair of products is thermodynamically most favored.

The internal substitution reaction of the α-anion **1** in Fig. 2 provides an attractive explanation of the observed fragments in that three major products are produced by only two carbon-bond fragmentation. However, the relative abundances of the products are in poor agreement with the calculated energy profile depicted in Fig. 2 which indicates that CN^- is the kinetically and thermodynamically preferred product ion, in contradiction to the experimental results shown in Fig. 1.

Alternative pathways, in which the fragments are formed by direct fragmentation from the β- and γ-anions **11** or **14**, were also investigated (Fig. 3). Only small barriers separate these ions from isomerizing into **1**. The isomerizations **1** → **11** and **1** → **14** correspond to entropically favorable intramolecular 1,5- and 1,4-proton shifts, respectively. In the latter case, a second energy barrier, represented by **TSG**, has to be surmounted before the molecular system ends up in the leftmost product region of Fig. 3, ultimately giving **18** (*m*/*z* 94) + **8** or **17** + **10** (*m*/*z* 40). Starting from **1** and moving to the right, we observe that isomer **11** may pass further on through **TSE** to give the products **13** + **4** (*m*/*z* 26). In full accordance with the experimental observations, passage to the left giving the ionic products **18** (*m*/*z* 94) and **10** (*m*/*z* 40) is preferred compared to passage to the right giving **4** (*m*/*z* 26). Moreover, the calculated higher acidity of **17** compared to **8** is also in agreement with the experiment, since the amount of **18** (*m*/*z* 94) is higher than

of **10** (*m*/*z* 40). We therefore conclude that the main reaction pathways leading to the fragments **4** (*m*/*z* 26), **10** (*m*/*z* 40) and **18** (*m*/*z* 94) are those of Fig. 3, rather than those of Fig. 2. This reaction which lead to formation of cyanide and acetonitrile anion can be regarded as proceeding by an E1cB mechanism in the which the anion is formed by an intramolecular proton transfer.

The right-hand side of Fig. 4 shows the potential energy profile relevant for the dissociation into the ions with *m*/*z* 52 and 82. The mechanism is straightforward in the sense that the rate determining step essentially is a γ-cleavage (via **TSI**). However, subsequent to passage of **TSI**, a hydrogen is transferred from the α-carbon to the nascent radical site at the terminal carbon. This "hidden" hydrogen rearrangement [22], results in the transient species **19**, that may dissociate into **21** (*m*/*z* 82) and **22**. Alternatively, it may transfer a proton between the two components of the complex to produce the short-lived intermediate **20** which ultimately dissociates into the products **23** and **24** (*m*/*z* 52). The high barrier for the γ-cleavage is in agreement with low abundance of *m*/*z* 52 and 82 in the MIKE-spectra of octanedinitrile anion (Fig. 1 and Table 1). The magnitudes of the translational energy releases in the reactions of the parent anions from FAB are also in agreement with the calculated reaction profiles. Formation of cyanide (*m*/*z* 26) has the highest translational energy release and is indeed formed via **TSE** which has more than five times the potential energy of the products **13** + **4**. The reactions shown in Fig. 3 give products via **TSI** with an energy barrier less than twice the product energy, and the products **18** + **8** and **17** + **10** are formed via **TSG** and **TSH** with energies comparable to that of the products. When CI is used to produce the anions, a fraction of them must have enough internal energy to cross the barrier at **TSI**. For this population the intramolecular substitution reactions of Fig. 2 is also available, but such reactions will be disfavored on the basis of bothersome entropy.

The left-hand side of Fig. 4 shows the isomerization of **1** into the Thorpe–Ziegler product **28** and the product of a 1,3-hydrogen rearrangement **29**. The latter is by far lower in energy than **1**, from which it is separated by a considerable barrier **TSM**.

As shown in Fig. 1b the peak at *m*/*z* 82 which can be assigned to **21** appears to have one wide and one narrow component when the parent anion is formed by CI. The two components differ by the magnitude of the translational energy release. The reaction profile in Fig. 4 is in agreement with such an observation. A bimodal translational energy release distribution can be observed when either two different reaction pathway are possible or when the internal energy distribution of reacting metastable ions is bimodal. In model calculations it has been shown that a reaction profile such as shown in Fig. 4 can lead to a bimodal distribution [23]. Formation of the low-energy non-reacting isomer in the source can provide a reservoir of highly energetic ions with the structure **29** which, owing to the two high barriers at **TSM** and **TSI**, may fragment with the same rate as ions with lower internal energy with the structure **1** which only have to cross one barrier at **TSI**. Thus the narrow component of the peak at *m*/*z* 82 is due to fragmentation of **1** into **21** and **22** whereas the broad component arises from the same product but from a population of **1** which has been produced by back-isomerization of **29**. The peak at *m*/*z* 52 assigned to acrylonitrile anion **24**, the other product at the right-hand side of Fig. 4, appears to be Gaussian. This may just be an indication of the different dynamics of the reaction leading to **23** and **24** compared to that which ends up with **21** and **22**. It is therefore likely that the high-energy population of **1** must contribute to all the observed fragments, but only when the distribution of the translational energy release is significantly different from that of the low-energy population, it will be noticed from the peak shapes. When the translational energy distributions of the two populations are similar the high-energy population only contributes to the greater peak-width noticed with CI.

If the explanation above is correct the absence of any composite peak in the FAB MIKE-spectrum indicate that **29** is not formed in significant abundance under FAB ionization. Ion production by FAB gives ions with generally little internal energy [24] and fewer

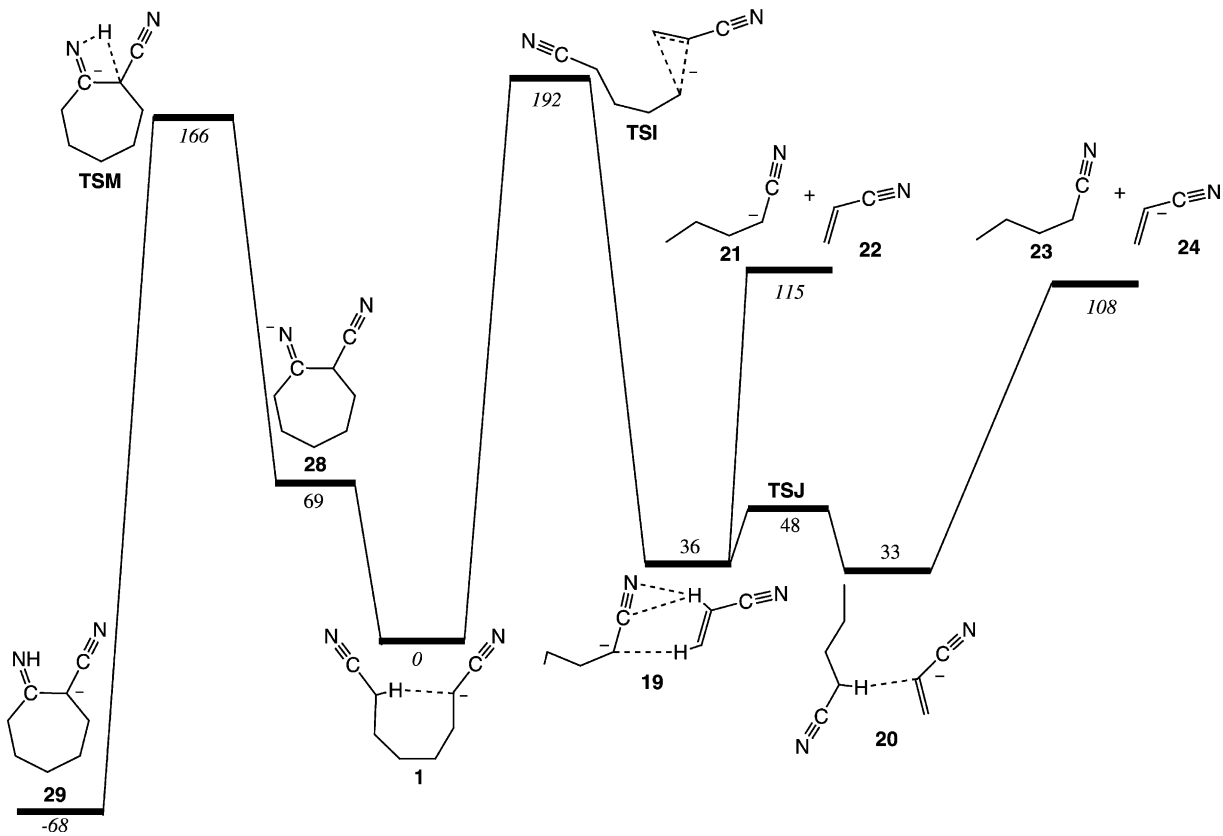

Fig. 4. Unimolecular reaction of octanedinitrile anion. Potential energy diagram for reactions giving ions with *m*/*z* 52 and 82. Number in italics correspond to QCISD-FC/6-311++G(d,p)//B3LYP/6-31G(d), while the numbers in regular font correspond to B3LYP/6-31G(d). Relative energies are given in kJ mol^{-1}.

high-energy ions will give a smaller population of **29** with sufficient energy to contribute to the reacting metastable ions.

In the MIKE-spectra of heptanedinitrile anion CN^- (*m*/*z* 26) is the only observed ionic fragment. As for the octanedinitrile anion discussed in detail above, the most stable isomer of this anion is formed by deprotonation of an α-position. In order to accommodate fragmentation into CN^-, it is necessary to form the intermediate where the β-hydrogen is removed. This can be obtained through a 1,4-proton shift. Loss of CH_2CN^-, on the other hand, would require transfer of a proton from the γ-position, which in this shorter molecule would have to go via a 1,3-proton shift—a mechanism which seems less likely both in terms of energy and entropy. This assumption is supported by our B3LYP/6-31G(d)//B3LYP/6-31G(d) calculations of the corresponding reactants, transition structures and products. The barrier for the 1,3-shift was calculated to be 77 kJ mol^{-1} higher than that of the 1,4-shift. Based on the results from the higher homologue, we would expect that this barrier is underestimated with B3LYP. Since heptanedinitrile as well as the longer-chained homologues can be cyclized by the Thorpe–Ziegler reaction, the marked differences between the fragmentation in the gas phase of the heptanedinitrile anion and the two homologues support the assumption made above that the gas-phase fragments are not formed via the Thorpe–Ziegler intermediate (Fig. 5).

The fragmentation of nonanedinitrile anion can be explained in parallel to that of the octanedinitrile

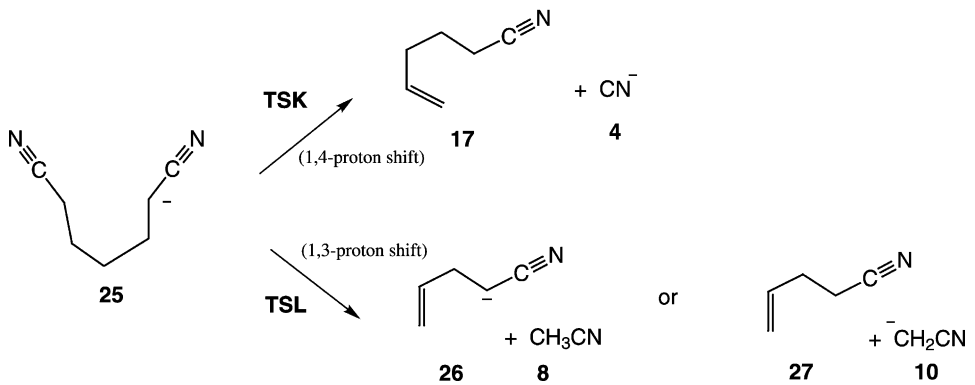

Fig. 5. Unimolecular reactions of heptanedinitrile anion.

anion. Its behavior is in every respect similar, of course with the exception that in the series of fragment ions some of the peaks have to be assigned to homologous ions. The analogous fragmentation pathway to that shown for octanedinitrile anion in Fig. 4 produces the fragments with *m*/*z* 96 and 52. The associated peaks are shown in Fig. 1c and d. In this case they are both composite, and their appearance can be explained in analogy to that of the peak at *m*/*z* 82 from octanedinitrile anion. The high-energy population of the homologue of **29** contributes to the wider peaks in the CI MIKE-spectra and in the case of nonanedinitrile anion both fragmentations on the right-hand side of Fig. 4 gives rise to composite peaks. Based on the obvious similarities between the experimental data for octane- and nonanedinitrile anion, we anticipate that their potential energy profiles are similar. The main difference in the reaction mechanism lies in the ring size of the cyclic transition structures. Thus the formation of the α- and β-carbanions (Fig. 3) which have five- and six-membered cyclic transition structures (**TSD** and **TSF** in Fig. 3) in the case of the octanedinitrile anion, will have six- and seven-membered cyclic transition structures for nonanedinitrile anion. **TSF** is close to the highest barriers leading the products. However, **TSD** lies significantly lower than **TSE** which is the highest barrier for the reaction leading to **4** (CN^-), and it is not obvious how the energy of this transition structure should depend on the chain-length. Similarly for the mechanism of the reaction shown on the right-hand side of Fig. 4 for which **TSI** the highest barrier.

When these changes in mechanism are correlated to the experimental results only the FAB MIKE-spectra are fully useful, since the CI MIKE-spectra may be complicated by the bimodal energy distribution of the reactant, as discussed above. In the FAB MIKE-spectra of octanedinitrile, the ionic fragments **24** (*m*/*z* 52) and **21** (*m*/*z* 82) formed via **TSI** have abundances of 16 and 12% (Table 1). For the nonanedinitrile anion the abundances of the equivalent fragments at *m*/*z* 52 and 96 are significantly lower. Thus for nonanedinitrile anion, the reactions shown in Fig. 3 are even more favored compared to those shown in Fig. 4 than in the case for octanedinitrile anion.

Acknowledgements

The authors wish to thank The Research Council of Norway (Programme for Supercomputing) and NOTUR (The Norwegian High Performance Computing Consortium) for computing time, The Danish Research Council for grant no. 9801751, and Steen Hammerum for valuable discussions.

References

[1] G.N. Merrill, G.D. Dahlke, S.R. Kass, J. Am. Chem. Soc. 118 (1996) 4462.

[2] R.A.L. Peerboom, L.J. de Koning, N.M.M. Nibbering, J. Am. Chem. Soc. Mass Spectrom. 5 (1994) 159.
[3] K.B. Wiberg, H. Castlejon, J. Org. Chem. 60 (1995) 6327.
[4] W.H. Saunders, J.E. Van Vertht, J. Org. Chem. 60 (1995) 3452.
[5] G. Bojesen, Unpublished (2003).
[6] H. Baron, F.G.P. Remfry, Y.F. Thorpe, J. Chem. Soc. 85 (1904) 1726.
[7] K. Ziegler, H. Eberle, H. Ohlinger, Ann. Chem. 504 (1933) 94.
[8] D.J. Burinsky, R.H. Cooks, J. Org. Chem. 47 (1982) 4864.
[9] M.J. Raftery, J.H. Bowie, Org. Mass Spectrom. 23 (1988) 719.
[10] M.A. Baldwin, P.J. Derrick, R.P. Morgan, Org. Mass Spectrom. 11 (1976) 440.
[11] R.G. Cooks, J.H. Beynon, R.M. Caprioli, G.R. Lester, Metastable Ions, Elsevier, Amsterdam, 1973.
[12] M.J. Frisch, et al., GAUSSIAN 98, Gaussian Inc., Pittsburgh, PA, 1998.
[13] A.D. Becke, J. Chem. Phys. 98 (1993) 5648.
[14] P.C. Hariharan, J.A. Pople, Theor. Chim. Acta 28 (1973) 213.
[15] J.A. Pople, M. Head-Gordon, K. Raghavachari, J. Chem. Phys. 87 (1987) 5968.
[16] J.E. Bartmess, in: P.J. Linstrom, W.G. Mallard (Eds.), NIST Chemistry WebBook, NIST Standard Reference Database Number 69 (http://webbook.nist.gov), National Institute of Science and Technology, Gaithersburg, MD, 2001.
[17] C.B. Lebrilla, C. Schulze, H. Schwarz, J. Am. Chem. Soc. 109 (1987) 98.
[18] S.L. Craig, M. Zhong, J.I. Brauman, J. Am. Chem. Soc. 121 (1999) 11790.
[19] S. Gronert, Chem. Rev. 101 (2001) 329.
[20] C.H. DePuy, J. Org. Chem. 67 (2002) 2393.
[21] J.K. Laerdahl, E. Uggerud, Int. J. Mass Spectrom. 214 (2002) 277.
[22] H. Schwarz, Top. Curr. Chem. 97 (1981) 1.
[23] S. Hammerum, T. Vulpius, H.-E. Audier, Org. Mass Spectrom. 27 (1992) 369.
[24] R. Hoogerbrugge, M. Bobeldejk, P.G. Kistemaker, J. Los, J. Chem. Phys. 88 (1988) 5314.